

# A Networked Modular Hardware and Software System for MRI-guided Robotic Prostate Interventions

Hao Su<sup>a</sup>, Weijian Shang<sup>a</sup>, Kevin Harrington<sup>a</sup>, Alex Camilo<sup>a</sup>, Gregory Cole<sup>a</sup>,  
Junichi Tokuda<sup>b</sup>, Nobuhiko Hata<sup>b</sup>, Clare Tempany<sup>b</sup>, and Gregory S. Fischer<sup>a</sup>

<sup>a</sup>Department of Mechanical Engineering, Worcester Polytechnic Institute, Worcester, USA;

<sup>b</sup>Department of Radiology, Brigham and Women's Hospital, Boston, USA

## ABSTRACT

Magnetic resonance imaging (MRI) provides high resolution multi-parametric imaging, large soft tissue contrast, and interactive image updates making it an ideal modality for diagnosing prostate cancer and guiding surgical tools. Despite a substantial armamentarium of apparatuses and systems has been developed to assist surgical diagnosis and therapy for MRI-guided procedures over last decade, the unified method to develop high fidelity robotic systems in terms of accuracy, dynamic performance, size, robustness and modularity, to work inside close-bore MRI scanner still remains a challenge. In this work, we develop and evaluate an integrated modular hardware and software system to support the surgical workflow of intra-operative MRI, with percutaneous prostate intervention as an illustrative case. Specifically, the distinct apparatuses and methods include: 1) a robot controller system for precision closed loop control of piezoelectric motors, 2) a robot control interface software that connects the 3D Slicer navigation software and the robot controller to exchange robot commands and coordinates using the OpenIGTLink open network communication protocol, and 3) MRI scan plane alignment to the planned path and imaging of the needle as it is inserted into the target location. A preliminary experiment with ex-vivo phantom validates the system workflow, MRI-compatibility and shows that the robotic system has a better than 0.01mm positioning accuracy.

**Keywords:** Magnetic resonance imaging, prostate biopsy, prostate brachytherapy, piezoelectric actuation, OpenIGTLink, image-guided therapy, MRI-guided intervention, MRI-compatible robot, surgical navigation.

## 1. INTRODUCTION

Subcutaneous needle, catheter and electrode placement are some of the most common minimally invasive procedures. Numerous tubular surgical tool applications, ranging from fine needle spinal anesthesia and sextant prostate biopsy with targeted tissue harvesting to microelectrode insertion in deep brain stimulation for Parkinson's disease, have capitalized the intrinsic minimally invasive feature and the attendant benefits including low cost, less morbidity and faster recovery comparing with many other diagnosis and therapies. However, conventional image-guided needle placement typically relies on static, previously acquired images. If intra-operative imaging is available, it is typically from computer tomography (CT) or fluoroscopy<sup>1</sup> which produces exposes patient and doctor to ionizing radiation and has poor soft tissue contrast, or from ultrasound which provides low quality images. MRI can provide high resolution multi-parametric imaging, large soft tissue contrast, and interactive image updates making it an ideal modality for cancer diagnosis and real-time surgical tools guidance. The rationale of deploying robotic systems inside MRI is to synergize the visual capability of MRI and the manipulation capability of robotic surgical assistance to guarantee high geometric accuracy with intra-operative image guidance. Considerable efforts have focused on robot-assisted surgery with ultrasound and CT guidance, while the last decade witnessed further significant efforts expended for MRI-guided robotic interventions.

There is an engineering tradeoff for actuation approach selection between intrinsic MRI compatibility and motor dynamic performance. Primarily, four actuation principles have been evaluated for MRI-guided interventions, namely remote actuation, hydraulic, pneumatic and ultrasonic/piezoelectric actuators. The first three

---

Further author information: (Send correspondence to Hao Su or Gregory Fischer, <http://aimlab.wpi.edu> )

Hao Su: E-mail: [haosu@wpi.edu](mailto:haosu@wpi.edu), Telephone: (1)508-831-5191

Gregory S. Fischer: E-mail: [gfischer@wpi.edu](mailto:gfischer@wpi.edu), Telephone: (1)508-831-5261

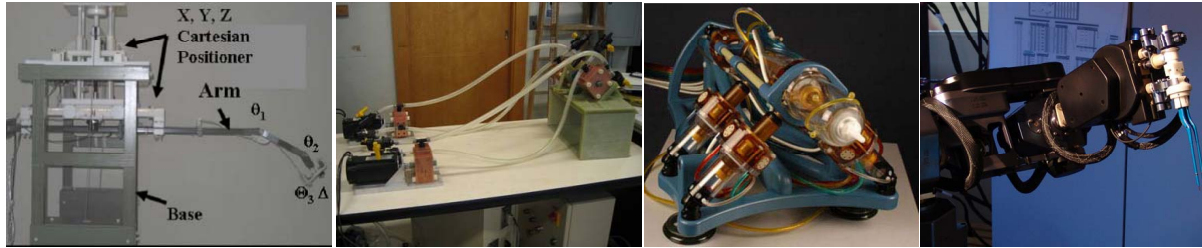


Figure 1. Four representative MRI guided surgical robots utilizing different actuation techniques, namely manual actuation,<sup>2</sup> hydraulic actuation,<sup>3</sup> pneumatic actuation<sup>4</sup> and piezoelectric actuation.<sup>5</sup>

methods are considered intrinsically MRI compatible for the reason that it involves no any metallic material by delicate design or system modification. However, remote actuation suffers from bulky structure, low bandwidth and lower resolution and is not preferable for robotic applications. Especially, it requires mental computation to localize surgical tool and align MRI scan plane, this non-coordinated motion for the user bears limited merit. Hydraulic and pneumatic actuation can completely avoid electrical and magnetic noise and the latter has been deployed in a number of systems. Due to cavitation and fluid leakage, hydraulic actuation is not preferred in medical environments.

Pneumatic and piezoelectric actuations are the primary armamentarium for robotic applications in MRI. Pneumatic actuation has been evaluated by several groups<sup>6-8</sup> and novel pneumatic step motors have been developed.<sup>9</sup> While pneumatic technology does have a very low level of image interference, it is extremely hard to model and control due to cylinder friction, especially for dynamic applications and some range servoing, which are frequently required for surgical applications. The scalability, simplicity, size and inherent robustness of electromechanical systems present a clear advantage over pneumatically actuated systems. Piezoelectric motors using commercially available motor controllers negatively impacted image quality. Fig. 1 illustrates four representative MRI guided surgical robots utilizing different actuation techniques, remote manual actuation,<sup>2</sup> hydraulic actuation,<sup>3</sup> pneumatic actuation<sup>4</sup> and piezoelectric actuation.<sup>5</sup>

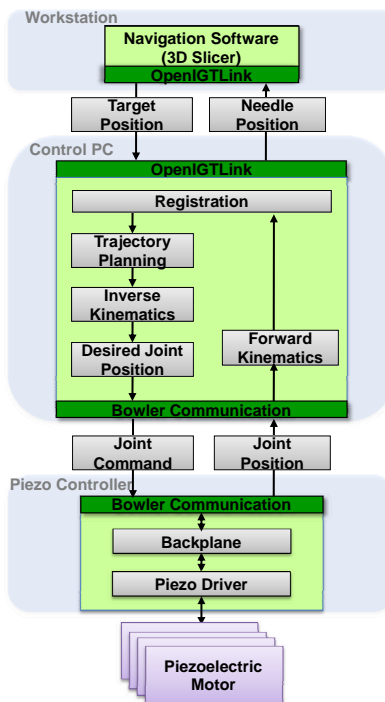


Figure 2. System architecture diagram shows the connection and data flow.

We have developed a plethora of proven MRI-compatible enabling technologies consisting of sensors, actuators, kinematic modules, software, and unified control system that provides a hardware and software toolbox that not only allows for simple MRI-compatible tool (e.g. injector or research tool), but also for rapid prototyping of MRI-compatible robotic systems. The system is based on the concept that modular components can be combined to develop application-specific modules (See Fig. 2). A single control system can be used to control a multitude of compact, low-cost application-specific manipulators. The developed piezoelectric actuation system is capable of driving commercially available piezoelectric motors inside the MRI scanner during live imaging with the best reported MRI compatibility reported to date.<sup>10–12</sup> The average signal noise ratio loss is limited to 5% during actuator motion inside 3T MRI scanner.

## 2. MATERIALS AND METHODS

### 2.1 System Concept and Architecture

The integrated system, shown in Fig.2, consists of four major components, namely: 1) high level navigation software 3D Slicer,<sup>13</sup> 2) robot control interface software, 3) robot controller for precision closed loop control of piezoelectric motors and 4) needle placement robot. Three-dimensional surgical navigation software 3D Slicer serves as a user interface to visualize and define target in patient coordinates (i.e. image space). The primary functionality of the robot control interface software is to organize system workflow, including robot calibration, fiducial registration, robot kinematics and robot motion control. The robot control interface software connects 3D Slicer and the robot controller to exchange robot commands using OpenIGTLink.<sup>14</sup> Communication from the robot control interface software to the robot controller is through a fiber optic Ethernet connection run through the MRI scanner room's patch panel wave guide. Being the only necessary connection between scanner and console room, this eliminates a large source of noise that is introduced when electrical signals are passed through the walls of the scanner room.

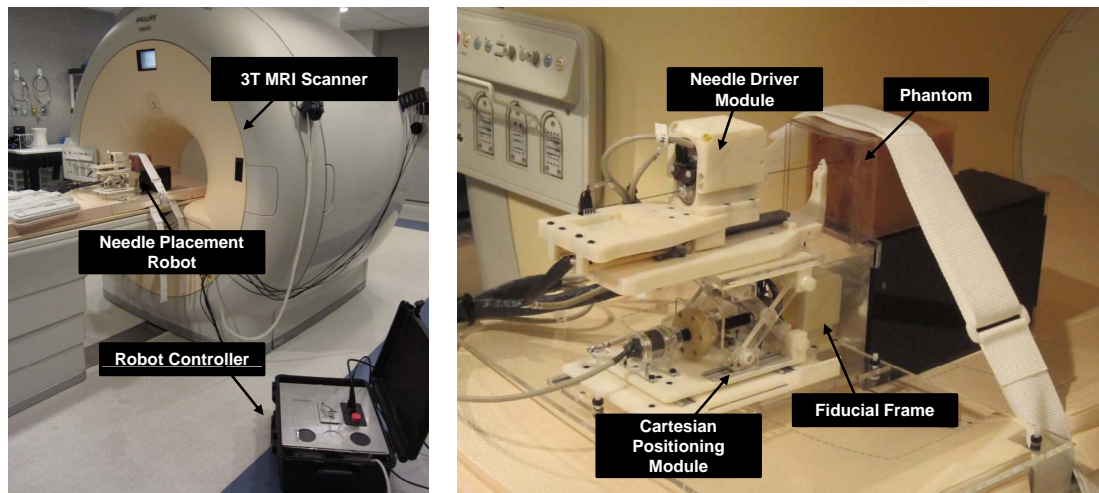


Figure 3. (Left) The prototype needle placement robot for percutaneous prostate interventions inside 3T MRI scanner and the robot controller is inside the scanner room beside the scanner, and (right) a detailed view of the robot with phantom inside MRI scanner.

### 2.2 Needle Placement Robot for Percutaneous Prostate Interventions

The robotic system is a MRI-compatible piezoelectric actuated robot for prostate brachytherapy with real-time in situ needle steering capability and fiber optic sensing in 3T MRI.<sup>15–18</sup> A steerable active cannula version of the MRI-compatible surgical robot is reported in.<sup>19</sup> The 6-degrees-of-freedom (DOF) robot consists of a modular 3-DOF needle driver with fiducial tracking frame and a 3-DOF actuated Cartesian stage. The needle

driver provides needle cannula rotation and translation (2-DOF) and stylet translation (1-DOF). Due to physical interaction between needle and soft tissue, the system utilizes piezoelectric actuation (PiezoMotor actuators, Uppsala, Sweden) for better accuracy, dynamic performance and robustness comparing with the pneumatic counterparts.<sup>20</sup> Optical encoders with differential signaling (US Digital, Vancouver, Washington) have been thoroughly tested in a 3T MRI scanner with satisfactory performance. Fig. 3 (left) illustrates the system setup inside scanner room while Fig. 3 (right) is a detailed view of the robot with phantom inside MRI scanner.

To avoid the problem with commercial piezoelectric drivers which usually induce high frequency RF noise inside scanner room, a new low noise driver as shown in Fig.4 was developed. A waveform synthesizer running on the FPGA is used to generate four independent motor-specific control waveforms of arbitrary phase and frequency. These control waveforms are then streamed out to the analog amplification stage at 25 mega samples per second.



Figure 4. Robot controller's motor driver that contains five piezoelectric driver boards. The custom control system resides in the shielded robot controller enclosure.

### 2.3 Surgical Navigation and Needle Tip Localization

The needle tip position in RAS (Right, Anterior, Superior) patient coordinates is based on the fiducial frame registration placed on the base of the robot to localize it within the scanner. The fiducial frame represents a Z shape and is made of seven tubes filled with high contrast agent. Multiple slices of the frame are used to calculate the position and orientation of the frame.

$$T_{Tip}^{RAS} = T_Z^{RAS} \cdot T_{Base}^Z \cdot T_{Rob}^{Base} \cdot T_{Tip}^{Rob} \quad (1)$$

Equation (1) shows the corresponding serial chain of transformations, where  $T_{Tip}^{RAS}$  is the needle tip in the patient coordinate system,  $T_Z^{RAS}$  is the fiducial in patient coordinates as determined by the Z-frame (fiducial frame) calibration,  $T_{Base}^Z$  is the mechanically fixed location of the fiducial on the robot,  $T_{Rob}^{Base}$  is the robot end effector location with respect to the robot base as determined from the forward kinematics of the robot, and  $T_{Tip}^{Rob}$  is the needle tip with respect to the end effector of the robot as determined by the encoder. In Slicer the planning software, a desired  $T_{Tip}^{RAS}$  is selected from the prostate image. The inverse kinematics is used to determine the actual needle position in patient coordinates which can then be pushed back up to Slicer for visualization.

### 2.4 System Workflow and Control Software

The workflow of the system that mimics traditional TRUS-guided prostate needle insertions is shown in Fig.5 (a). This workflow includes six states of operation and follows a coherent procedure. Comparing with our previous effort,<sup>21</sup> this software shown in Fig. 6 is more flexible, reconfigurable, and allows control of the robot from both task space (patient coordinates) and joint space.

Fig.7 illustrates two examples of communication methods using TCP and serial port between the control computer and the controller (motor driver) backplane. This enables system debug with serial port, and also enables

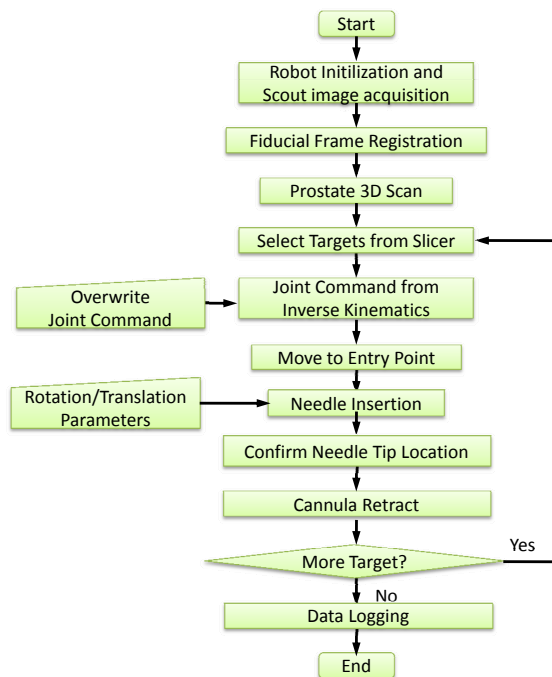


Figure 5. Workflow of MRI-guided needle placement that mimics that of traditional TRUS-guided prostate needle intervention.

networked connection for remote control and teleoperation. The backplane runs robot controller for planning and kinematics computation, and the backplane utilizes Serial Peripheral Interface (SPI) bus for communication with motor driver. The driver boards include a high power output amplification stage, which passes the signals from four linear amplifiers out to the actuators through  $\pi$  filters to further remove high frequency noise. Stall detection is implemented as a safety mechanism to detect joint limits and the motor joint would stop motion after 10ms.



Figure 6. Robot control interface software.

The system component of the control software follows the workflow and enables the following six modules to function in sequence.

- **System Initialization.** The hardware and software system is initialized. In this state, the operator prepares the robot by connecting the robot controller and attaching sterilized needle to the robot. The robot is calibrated to a pre-defined home position and loads the robot configuration from an XML file.
- **Planning.** Pre-operative MR images are loaded into the 3D Slicer. Targets are selected or imported into the Slicer platform.
- **Calibration.** A series of transverse images of the fiducial frame are acquired. Multiple images are used to perform multi-slice registration to enhance system accuracy.
- **Targeting.** Needle target is selected from the Slicer software and this desired position is transmitted to the robot to process inverse kinematics and the calculated joint command is used to drive piezoelectric motors. Targets or adjustments may also be directly entered or adjusted in the robot control interface software. Real-time MR images can be acquired during insertion that enables visualization of the tool path.
- **Verification.** The robot forward kinematics calculates actual needle tip position (from encoder measurements and registration results) which is displayed in the 3D Slicer. Post insertion MR images are acquired and displayed with overlaid target and actual robot position.
- **Emergency.** Both software and hard electrical stops are introduced in this state.

The safety of needle placement is ensured through several means that are implemented in software, electrical and mechanical levels: forces exerted by the piezoelectric motors are limited by the software (limits on drive frequency) and hardware (adjustable friction drive); insertion speeds are intentionally limited by setting a maximum drive frequency regardless of user input; positioning-sensing redundancy between onboard sensors and image-based localization; and emergency stops at several accessible locations, including an operator pendant.

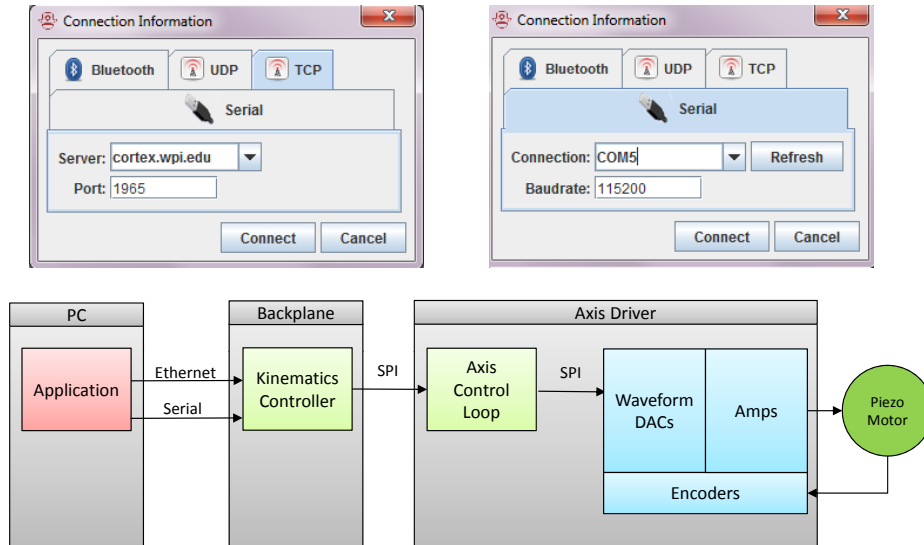


Figure 7. (Top) two illustrative examples of communication methods using TCP and serial communication between the control computer and the controller backplane. (Bottom) software robot communication modules.

### 3. EXPERIMENTAL RESULTS

Ex-vivo phantom experiments validate the system workflow, MRI-compatibility and system accuracy assessment. The preliminary results show that signal noise ratio reduction is less than 5% when the robot is running during MRI imaging.



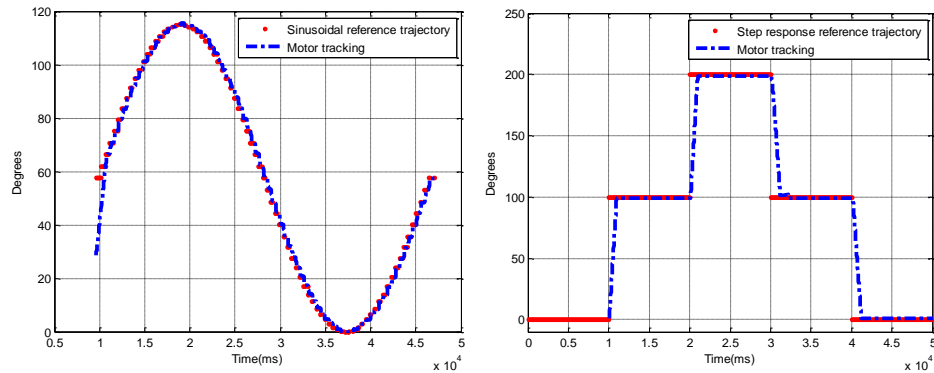


Figure 8. Motor position (blue) and set point (red) plotted against time in a sinusoid (left) and step response (right) experiment.

To assess the joint space accuracy of the piezoelectric actuation system, the control parameters (i.e. gains) were individually tuned for the best positioning accuracy. Based on the mechanical model of the piezoelectric actuator,<sup>22</sup> proportional-integral (PI) controller was used for each axis. Resolution of the linear quadrature optical encoders integrated into the robot is 0.0127 mm/count (0.0005" resolution). A digital dial gauge with the same resolution is utilized for independent measurement, where both the robot and the dial gauge are rigidly mounted on a fixture table. Each linear axis of robot (outer, middle and inner tube) is commanded to move in 1mm increments 40 times and the relative change in dial gauge reading is recorded. Based on independent measurement (which includes deflection, misalignment, etc.), the joints can be reliably controlled to within 30 $\mu$ m.

Also it shows that the robotic system has no larger than 0.02mm single axis tracking error as shown in Fig. 8, while the multi-slice registration has no larger than 0.27mm error.

## 4. CONCLUSION

This paper presented an integrated modular hardware and software system to enhance surgical outcome of intra-operative MRI-guided percutaneous prostate interventions. To enable straightforward control of various piezoelectric actuator types, while avoiding image quality degradation due to noisy drive electronics, a modular driver is developed to control piezoelectric motors and interpret optical encoders. A modular robot control interface software is used to organized system workflow and it connects MRI scanner, the Slicer open-source navigation and 3D visualization software, and the robot controller to exchange robot commands and coordinates using the OpenIGTLink. The accuracy of image-guided needle placements of multiple targets would be reported in the full manuscript.

## 5. ACKNOWLEDGEMENTS

This work is supported in part by the Congressionally Directed Medical Research Programs Prostate Cancer Research Program (CDMRP PCRP) New Investigator Award W81XWH-09-1-0191 and NIH awards 5P41RR019703, 5P01CA067165, 1R01CA111288.

## REFERENCES

- [1] Walsh, C. J., Hanumara, N. C., Slocum, A. H., Shepard, J.-A., and Gupta, R., "A patient-mounted, telerobotic tool for CT-guided percutaneous interventions," *Journal of Medical Devices* **2**(1), 011007 (2008).
- [2] Tsekos, N. V., Khanicheh, A., Christoforou, E., and Mavroidis, C., "Magnetic resonance-compatible robotic and mechatronics systems for image-guided interventions and rehabilitation: a review study," *Annu Rev Biomed Eng* **9**, 351–387 (2007).
- [3] Williams, D., *A Robot for Wrist Rehabilitation*, Master's thesis, Massachusetts Institute of Technology, USA (2001).

- [4] Stoianovici, D., Stoianovici, D., Patriciu, A., Petrisor, D., Mazilu, D., and Kavoussi, L., "A new type of motor: Pneumatic step motor," *Mechatronics, IEEE/ASME Transactions on* **12**(1), 98–106 (2007).
- [5] Sutherland, G. R., Latour, I., Greer, A. D., Fielding, T., Feil, G., and Newhook, P., "An image-guided magnetic resonance-compatible surgical robot.," *Neurosurgery* **62**, 286–92; discussion 292–3 (Feb 2008).
- [6] Yang, B., Tan, U., Gullapalli, R., McMillan, A., and Desai, J., "Design and Implementation of a Pneumatically-Actuated Robot for Breast Biopsy under Continuous MRI," *IEEE ICRA 2011 International Conference on Robotics and Automation* (2011).
- [7] Song, S.-E., Cho, N., Tokuda, J., Hata, N., Tempny, C., Fichtinger, G., and Iordachita, I., "Preliminary evaluation of a MRI-compatible modular robotic system for MRI-guided prostate interventions," *Biomedical Robotics and Biomechanics (BioRob), 2010 3rd IEEE RAS and EMBS International Conference on*, 796–801 (2010).
- [8] Song, S. E., Seifabadi, R., Krieger, A., Tokuda, J., Fichtinger, G., and Iordachita, I., "Robotic System for MRI-guided Prostate Intervention: Feasibility Study of Tele-operated Needle Insertion," *Computer Aided Radiology and Surgery* (2011).
- [9] Stoianovici, D., Song, D., Petrisor, D., Ursu, D., Mazilu, D., Muntener, M., Mutener, M., Schar, M., and Patriciu, A., "MRI Stealth robot for prostate interventions.," *Minim Invasive Ther Allied Technol* **16**(4), 241–248 (2007).
- [10] Su, H., Zervas, M., Cole, G., Furlong, C., and Fischer, G., "Real-time MRI-Guided Needle Placement Robot with Integrated Fiber Optic Force Sensing," *IEEE ICRA 2011 International Conference on Robotics and Automation* (2011).
- [11] Su, H. and Fischer, G. S., "High-field MRI-Compatible needle placement robots for prostate interventions: pneumatic and piezoelectric approaches," *Advances in Robotics and Virtual Reality*, Springer-Verlag (2011).
- [12] Cole, G., Harrington, K., Su, H., Camilo, A., Pilitsis, J., and Fischer, G., "Closed-Loop Actuated Surgical System Utilizing Real-Time In-Situ MRI Guidance," *12th International Symposium on Experimental Robotics - ISER 2010* (Dec 2010).
- [13] Pieper, S., Halle, M., and Kikinis, R., "3D Slicer," *Biomedical Imaging Nano to Macro, IEEE International Symposium on*, 632 – 635 (2004).
- [14] Tokuda, J. and Fischer, G., "OpenIGTLink: an open network protocol for image-guided therapy environment," *Int J Med Robot* **5**, 423–34 (Dec. 2009).
- [15] Su, H., Shang, W., Cole, G., Harrington, K., and Gregory, F. S., "Haptic system design for MRI-guided needle based prostate brachytherapy," *IEEE Haptics Symposium 2010*, IEEE, Boston, MA, USA (2010).
- [16] Su, H., Camilo, A., Cole, G., Hata, N., Tempny, C., and Fischer, G., "High-field MRI compatible needle placement robot for prostate interventions," *Proceedings of MMVR18 (Medicine Meets Virtual Reality)* (2011).
- [17] Su, H., Iordachita, I. I., Yan, X., Cole, G. A., and Fischer, G. S., "Reconfigurable mri-guided robotic surgical manipulator: Prostate brachytherapy and neurosurgery applications," *Engineering in Medicine and Biology Society, EMBC, Annual International Conference of the IEEE*, 2111 –2114 (2011).
- [18] Su, H., Zervas, M., Furlong, C., and Fischer, G., "A miniature MRI-compatible fiber-optic force sensor utilizing fabry-perot interferometer," *SEM Annual Conference and Exposition on Experimental and Applied Mechanics* (2011).
- [19] Su, H., Cardona, D., Cole, G., Webster III, R., and Fischer, G., "A MRI-Guided Concentric Tube Continuum Robot with Piezoelectric Actuation: A Feasibility Study," *IEEE ICRA International Conference on Robotics and Automation* (2012).
- [20] Fischer, G. S., Iordachita, I. I., Csoma, C., Tokuda, J., DiMaio, S. P., Tempny, C. M., Hata, N., and GaborFichtinger, "MRI-Compatible Pneumatic Robot for Transperineal Prostate Needle Placement," *IEEE/ASME Transactions on Mechatronics* **13**(3) (2008).
- [21] Tokuda, J., Fischer, G. S., DiMaio, S. P., Gobbi, D. G., Csoma, C., Mewes, P. W., Fichtinger, G., Tempny, C. M., and Hata, N., "Integrated navigation and control software system for MRI-guided robotic prostate interventions," *Computerized Medical Imaging and Graphics* **34**(1), 3 – 8 (2010).
- [22] Merry, R., Maassen, M., van de Molengraft, M., van de Wouw, N., and Steinbuch, M., "Modeling and waveform optimization of a nano-motion piezo stage," *Mechatronics, IEEE/ASME Transactions on* **16**(4), 615 –626 (2011).